INTERNATIONAL ATOMIC ENERGY AGENCY
UNITED NATIONS EDUCATIONAL, SCIENTIFIC AND CULTURAL ORGANIZATION

INTERNATIONAL CENTRE FOR THEORETICAL PHYSICS
34100 TRIESTE (ITALY) - P.O.B. 586 - MIRAMARE - STRADA COSTIERA 11 - TELEPHONE: 2240-1
CABLE: CENTRATOM - TELEX 460892-I

SMR/348 - 12

EXPERIMENTAL WORKSHOP ON
HIGH TEMPERATURE SUPERCONDUCTORS
(11 - 22 April 1988)

ON THE STRUCTURE OF PEROVSKITES AND INTRODUCTION OF LOWER DIMENSIONALITY

P. GANGULY
Solid State and Structural Chemistry Unit
Indian Institute of Science
560 012 Bangalore
India

PG I 1

ON THE STRUCTURE OF PEROVSKITES AND INTRODUCTION OF LOWER DIMENSIONALITY

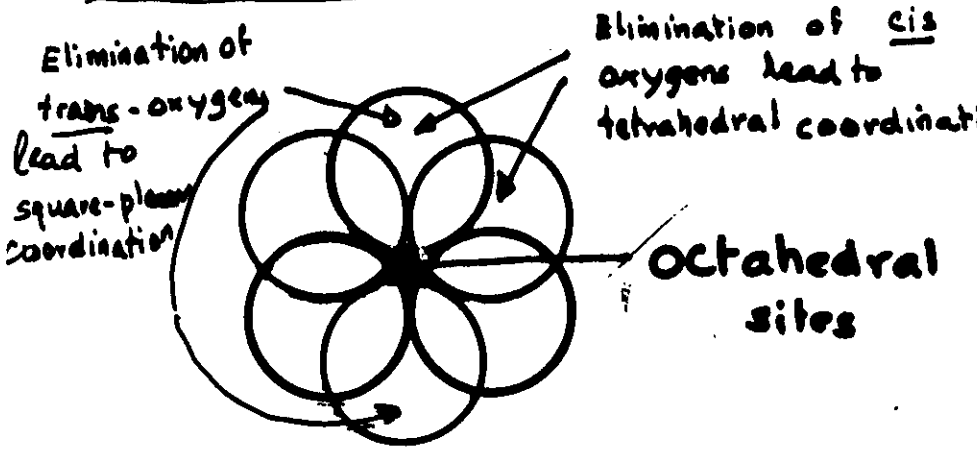

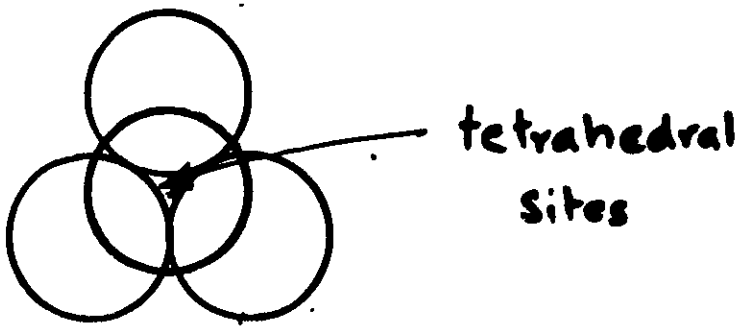

In ABO_3 perovskites octahedral sites made up only from oxide ions are occupied by B ions

AX_3 Tetrahedral sites always have one A -ation and hence such sites cannot be occupied by a B cation

PG I 2

close-packed spheres of anions (or atoms)

e.g. fcc structure obtained from cubic close packing. If this sheet is considered as A then next sheet of anions (atoms) could be centred on B or C sites to give B or C sheets.

Sequence ... ABCABCABC... is simple fcc

Sequence ... ABABAB... is hexagonal

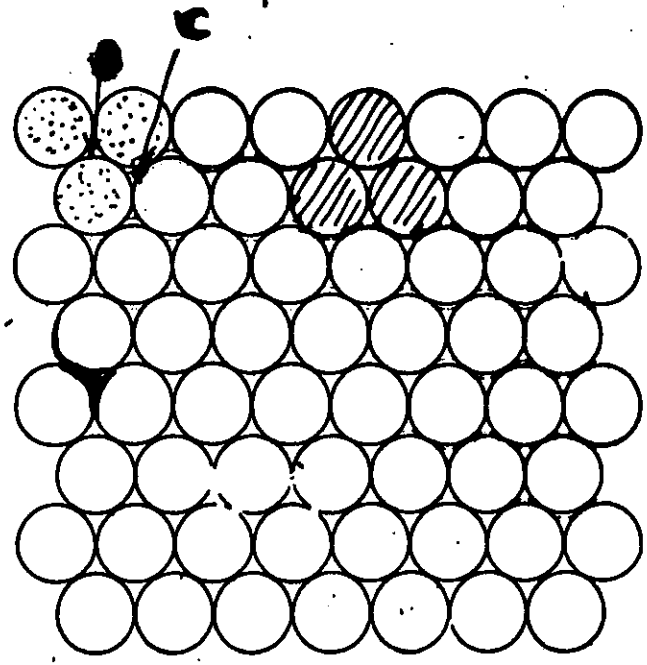

..... obtained by change of sequence ... ABCABABABCABCABABABC...

close-packed spheres of anions (or atoms)

e.g. fcc structure obtained from cubic close packing. If this sheet is considered as A then next sheet of anions (atoms) could be centred on B or C sites to give B or C sheets.

Sequence ...ABCABCABC... is simple fcc

Sequence ...ABABAB... is hexagonal

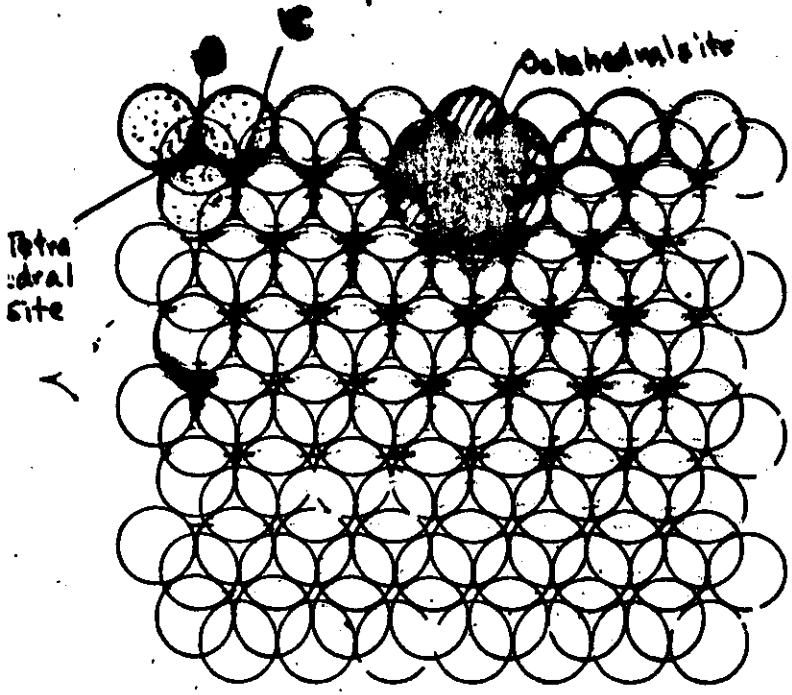

Different occupancy of tetrahedral or octahedral sites give rise to different structural types as in spinels and monorides

obtained by change of sequence ...ABCABABABCABCABABABC...

In perovskites ABX3 there is close-packing of A and X ions which have nearly similar size. Thus

showing occupancy of octahedral sites by Bion

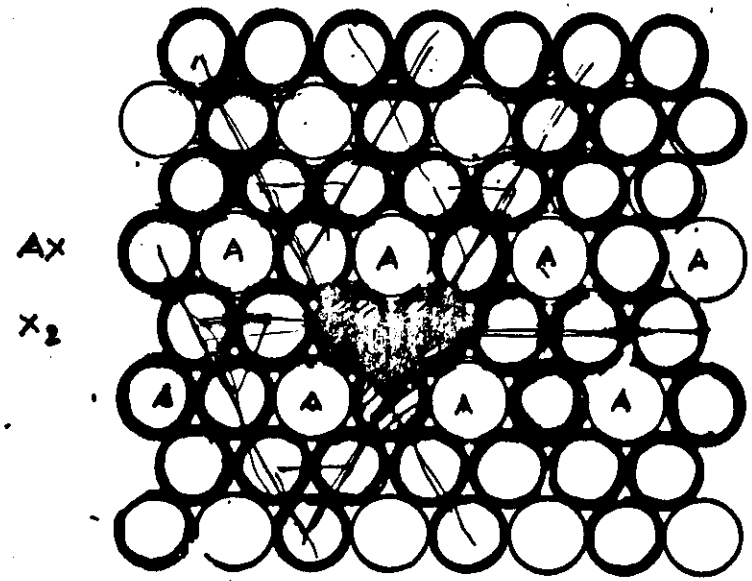

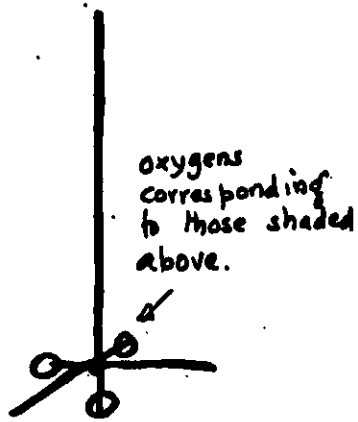

showing occupancy of octahedral sites

Bion

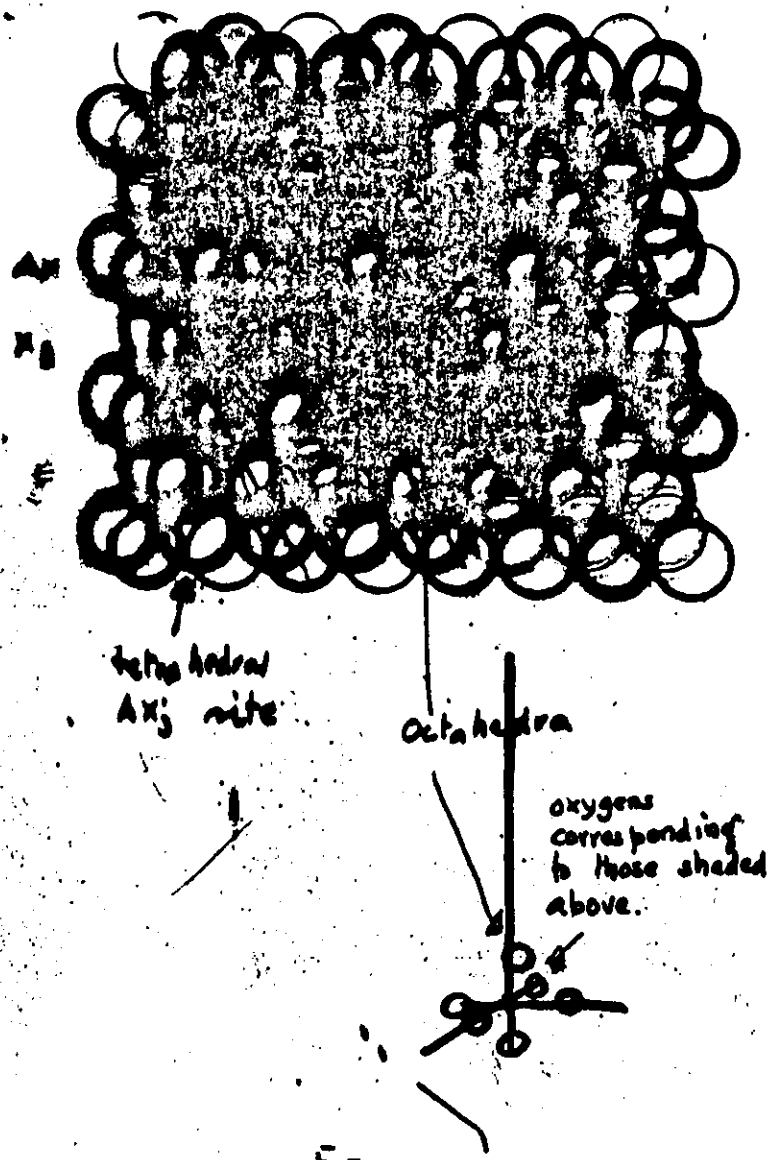

ABX_3 perovskite

see J B Goodenough J M Longo
Landolt Börnstein Tabellen Neuserics III /4a
Springer Verlag.

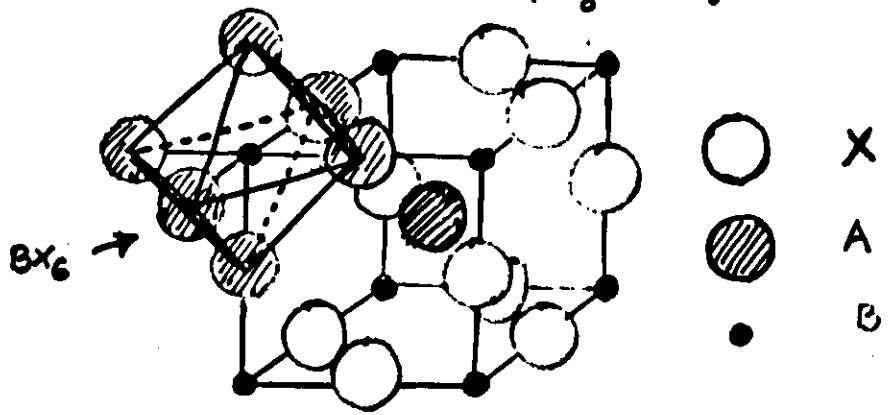

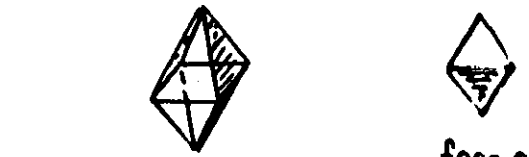

BX_6 octahedra

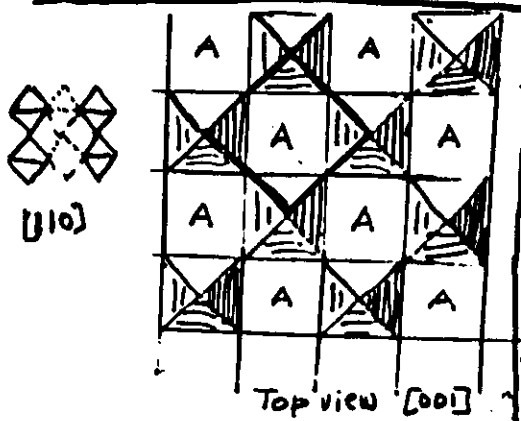

EXTENDED BX_6
octahedral Network

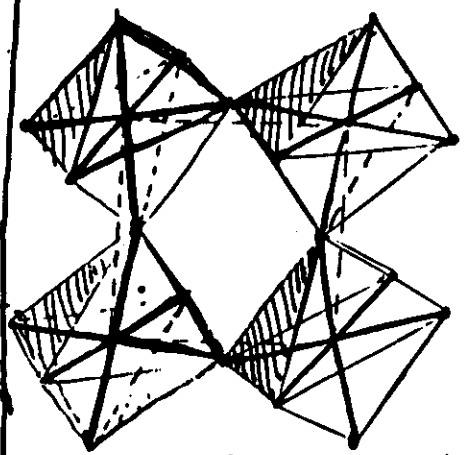

Tilting of BX_6 octahedra
B-X-B angle $\neq 180°$

PEROVSKITES

ABX_3

e.g. fluorides

$KNiF_3$, $KCuF_3$, $KMnF_3$ etc.

□ MnF_3, □ CuF_3, □ VF_3.

B ion has valency 2 & 3.

OXIDES

□ WO_3 — B^{6+}

$KTaO_3$ } B^{5+}

□ NbO_2F }

$SrTiO_3$ — B^{4+}

$LaFeO_3$ — B^{3+}

From ferroelectric ($BaTiO_3$) to metal.

Layered Perovskites

$(P_yZ_t)_n(ABX_3)_m$ Lanthanum $La_2CuO_{4.25}$ $La_4Cu_3O_{10}$

A□ $(ABX_3)_m$ K_2NiF_4, $K_3Ni_2F_7$

$(A'_2X_4)(A_{n-1}B_nX_{3n+1})$ Aurivillius phases.

CATION DEFICIENCY

ANION DEFICIENCY, EXCESS.

Some Ways to Tilt Octahedra

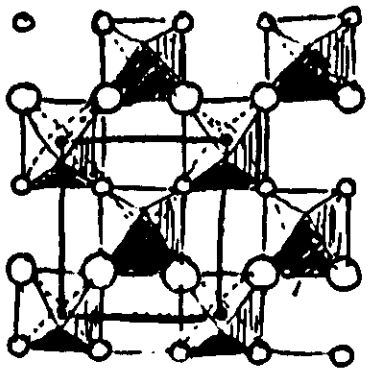

$\sqrt{2}$ increase in unitcell parameters

$a=b$

Tilting along 110 axis

○ above plane

o below plane

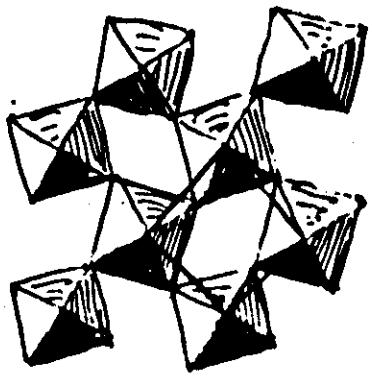

Rotation of octahedra along ≤ axis

$a=b$

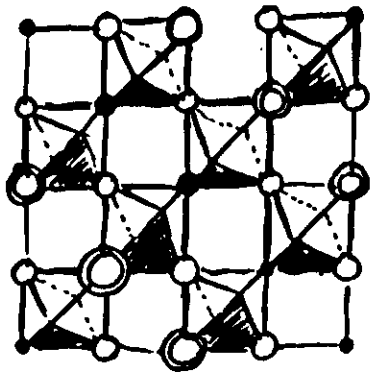

$a \neq b$

◎ above plane of paper

○ in plane of paper

• below plane

Tilting along 100 or 010 axes

B-X-B interaction different along the two direction

ANION DEFICIENCY IN PEROVSKITES

$ABO_{3-\delta}$

corner-shared polyhedral network

$\delta = 0$ all BX_6 octahedra

When $\delta \neq 0$ B coordination decreases

BX_5 or BX_4

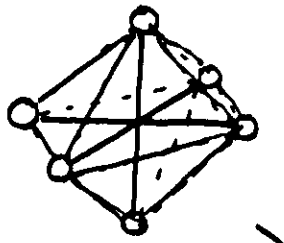

Octahedral

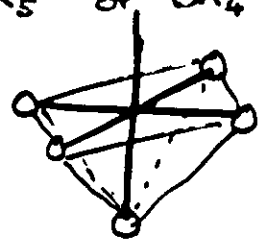

Square-pyramid BX_5

Mn^{3+}, Cu^{2+}

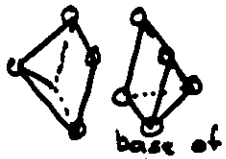

base of sq. pyramid must be facing each other

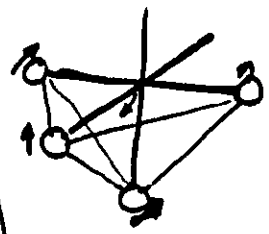

tetrahedral

Co^{2+}, Fe^{3+}

Top view

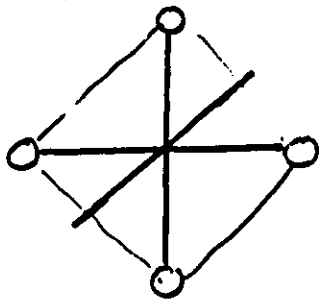

Square-planar

Cu^{2+}, Pd^{2+} etc.

octahedra	tetrahedra

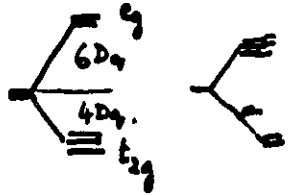

Cu^{3+} stabilised most t_{2g}^3 in octahedra

Fe^{3+} both oct. & Tet.

Co^{2+} d^7 stabilised best in tetrahedra.

Jahn-Teller ions

Mn^{3+} $t_{2g}^3 e_g^1$ prefer

Cu^{2+} $t_{2g}^6 e_g^3$ non-cubic symmetry

∴ sq. pyramidal or sq. planar

COMPOUNDS SUCH AS $CaFe^{4+}O_3$, $CaMn^{4+}O_3$ $SrCo^{4+}O_3$, $LaNi^{3+}O_3$ etc. are unstable to heating and lose oxygen

$CaFeO_3 \rightleftharpoons Ca_2Fe_2O_5 + O_2$ etc

$CaMnO_3 \rightarrow Ca_2Mn_2O_5$ through several stages.

Energy Levels of $3d^n$ ions in TiO_2

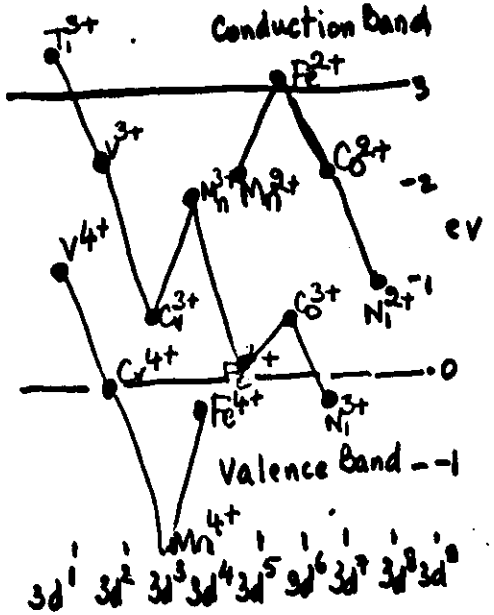

Ions with $3d^n$ levels in valence band are unstable

$M^{n+} + O^{2-} \rightleftharpoons M^{(n-1)+} + O^-$

$2O^- \rightleftharpoons O_2^{2-}$ (peroxide)

$O_2^{2-} \rightleftharpoons O_2 + 2e$

peroxides are known to decompose easily

cis-elimination of oxygen

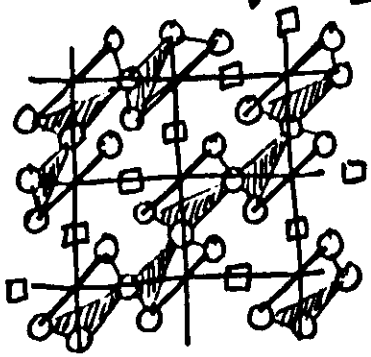

Tetrahedral Sheet alternates with sheets of all octahedral coordination

$Ca_2Fe_2O_5$

Brown. millerite

OTOTOTOT

planes of tetrahedra alternating with planes of octahedra (not shown)

general $A_nB_nO_{3n-1}$

$Ca_{4-x}Fe_3O_8$ $(Ca_4(Y))Fe_3O_{13}$

$Ca_4Fe_2Ti_2O_{11}$ $n=2, n=3$

Trans. elimination of oxygen

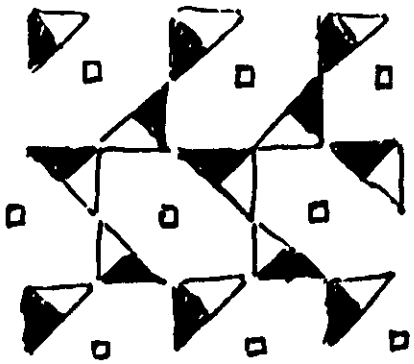

$Ca_2Mn_2^{3+}O_5$

only sq. pyramids

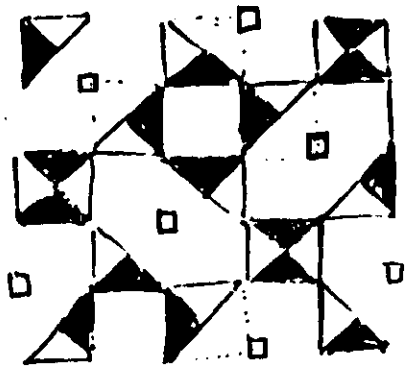

$(La,Ba)_2Cu_2O_{5.2}$

$La_4BaCu_5O_{13}$

sq. pyramids + octahedra.

PGI 10

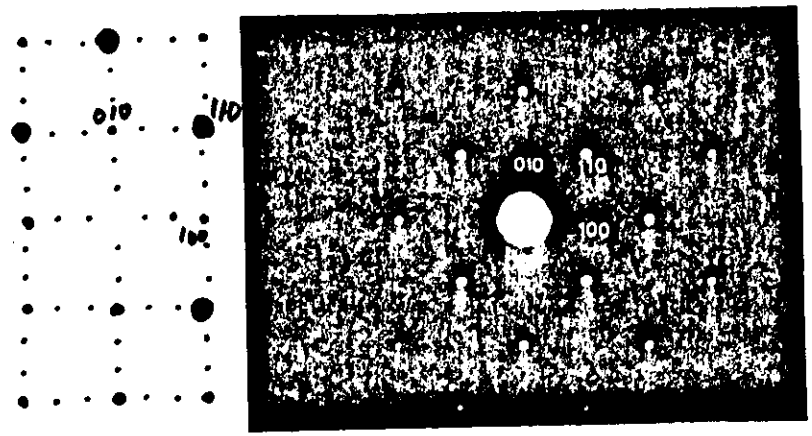

FIG. 8. Electron diffraction pattern of the H.T., X-ray cubic sample. Zone axis [001]$_c$. Notice the spot at the center of the reciprocal cubic cell (compare with Fig. 2) and the presence of two threefold superlattices along both β_{100} and β_{110}.

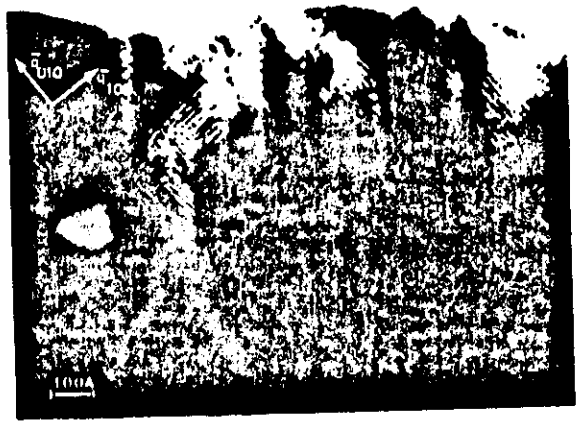

FIG. 9. Electron micrograph of the H.T., X-ray cubic sample, in the [001]$_c$ orientation of Fig. 8. The presence of microdomains, in which the perovskite cell is trebled in one of two perpendicular directions, is evident.

See Grenier JSSC.

P61 11

tion study of
/s that under
sitional varia-
means of the
nal microdo-

rrite was pre-
etric mixture
$9H_2O$), but in
s samples the
lved in dilute
: then decom-
/, after grind-
red at 1300°C.
de (L.T.) was
ntrolled oxy-
sphere (p_{O_2} =
the formation

de (H.T.) was
°C in air for 1
:hing down to

:rized by pow-
–Hägg pattern
emical analy-
rage oxidation
dilution in 3 *N*
's salt).
d diffraction
ens Elmiskop
sonically dis-
transferred to

$a_2LaFe_3O_8$

fraction work
ars to have an
a perovskite
:rs are a_p =

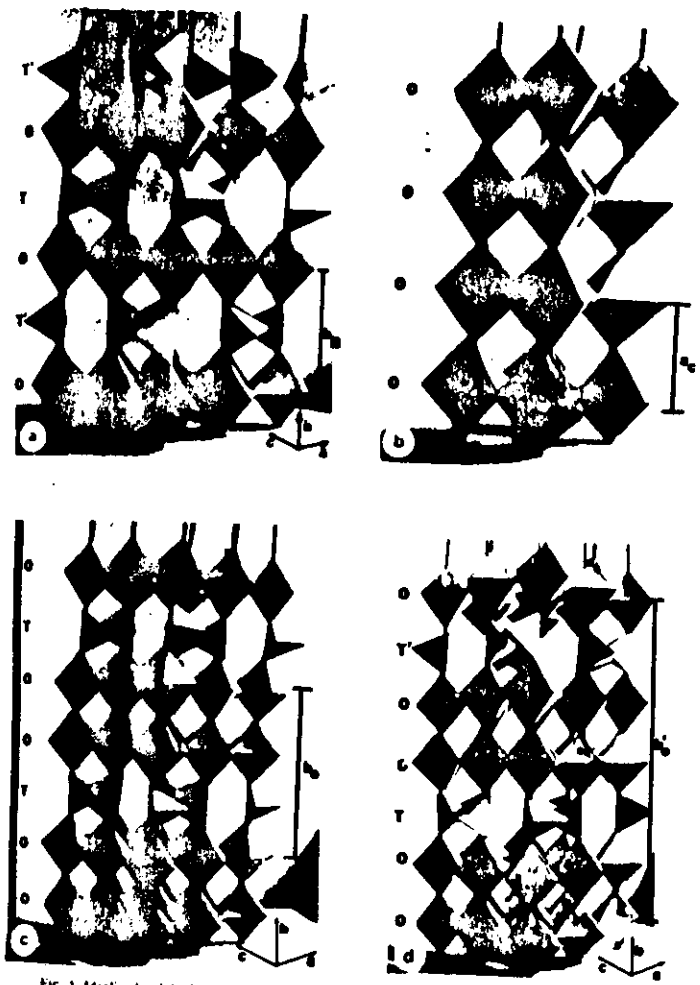

FIG. 1. Idealized polyhedral models of the following structures: (a) brownmillerite; (b) perovskite; (c) polytype I of $Ca_2LaFe_3O_8$; and (d) polytype II of $Ca_2LaFe_3O_8$.

P61 12

relevant to domain formation in perovskites of copper

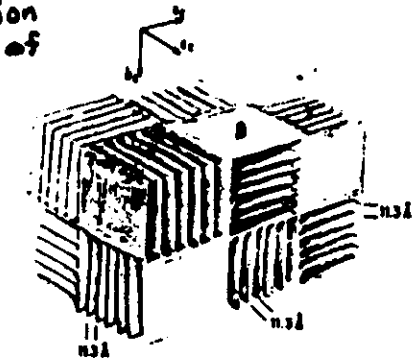

FIG. 13. Schematic representation of the intergrowth of three sets of domains which form the texture of the H.T. sample.

. X-ray cubic
ic perovskite
attice results,
et of domains
$a_p\sqrt{2} \times a_p 2 \times$

seen on the set
the unit cell is

afirm that the
base of the cal-
$_{1.67}La_{0.33}FeO_{2.67}$,
series of anion-
ural formulation
icular case A =
$\frac{3}{4}$ x = $\frac{3}{4}$ in the
ation, y = 1/n.
diffraction dia-
scopic observa-
the occurrence

of some disorder along the b_p axis, parallel to the cubic perovskite b_c axis. As clearly shown in Fig. 6 by electron microscopy, the existence of fringe spacings larger than required by the b_p = 11.29-Å dimension was often observed. The appearance of such a

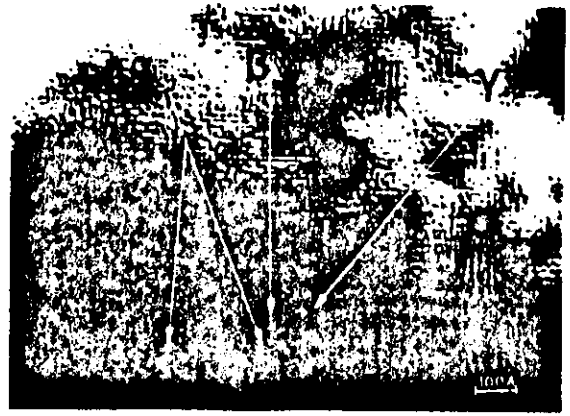

FIG. 14. Electron micrograph of the H.T. sample along the [001]$_c$ orientation showing the three sets of microdomains.

ANION DEFICIENCY IN A SITE

PGI 13

vacant oxides

$WO_{3-\delta}$

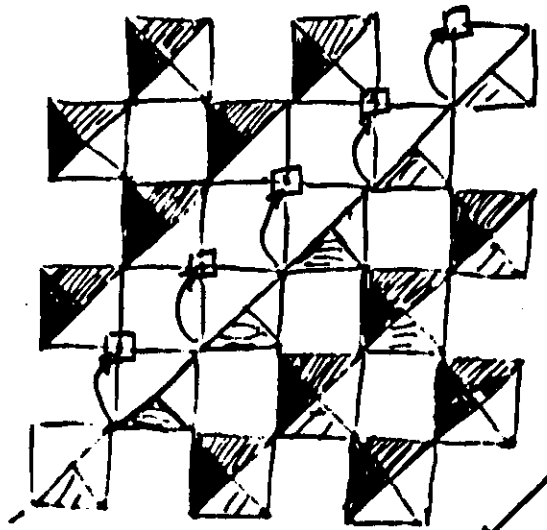

Crystallographic shear planes

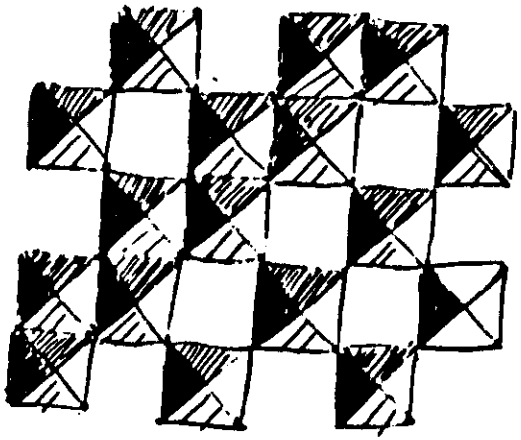

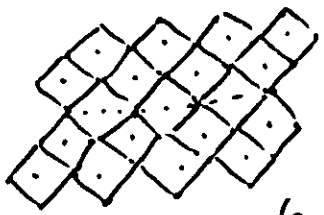

Y deficient

$YBa_2Cu_3O_7$

shows such intergrowths

$SrCu_2O_2$ $(CaCu_2O_3)$

$(SrCu_2O_2 + SrO)$

PGI 14

polytypism

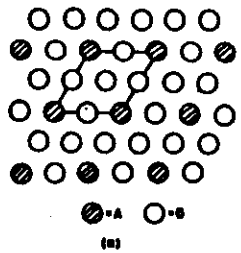

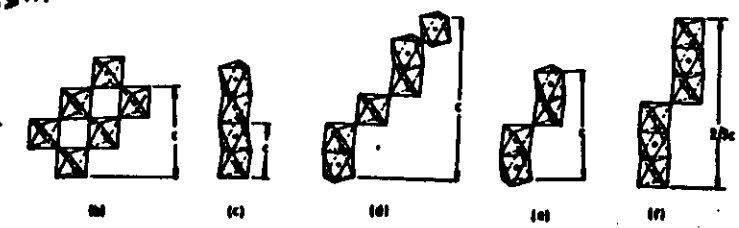

Fig. 2—(a) Close-packed AO_3 layer in perovskites; (b-f) BO_6 octahedra in different perovskite polytypes: (b) 3C; (c) 2H; (d) 6H; (e) 4H; and (f) 9R.

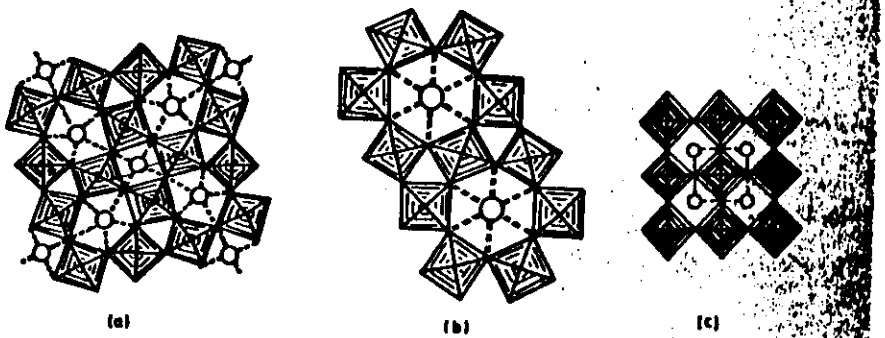

Fig. 3 Tungsten bronze structures: (a) tetragonal tungsten bronze (TTB); (b) hexagonal tungsten bronze (HTB); and (c) perovskite tungsten bronze (PTB).

PGI 15

Layered Perovskites

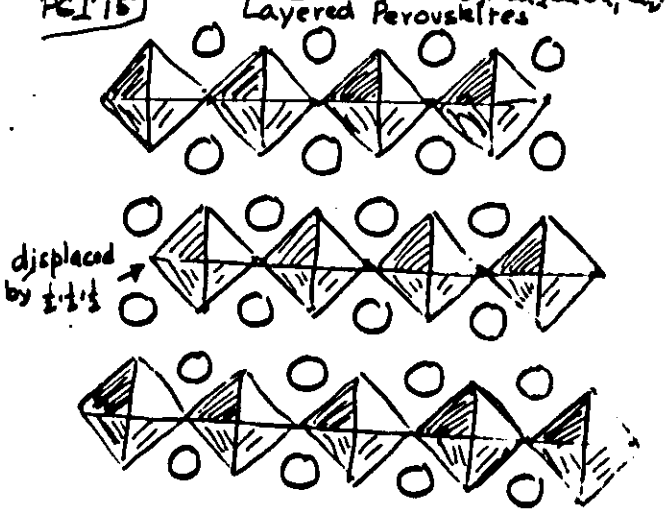

in general

$AO(ABO_3)_n$

evolution of magnetic and electrical properties with dimensionality

eg $SrO(La_{1-x}Sr_xMnO_3)_n$

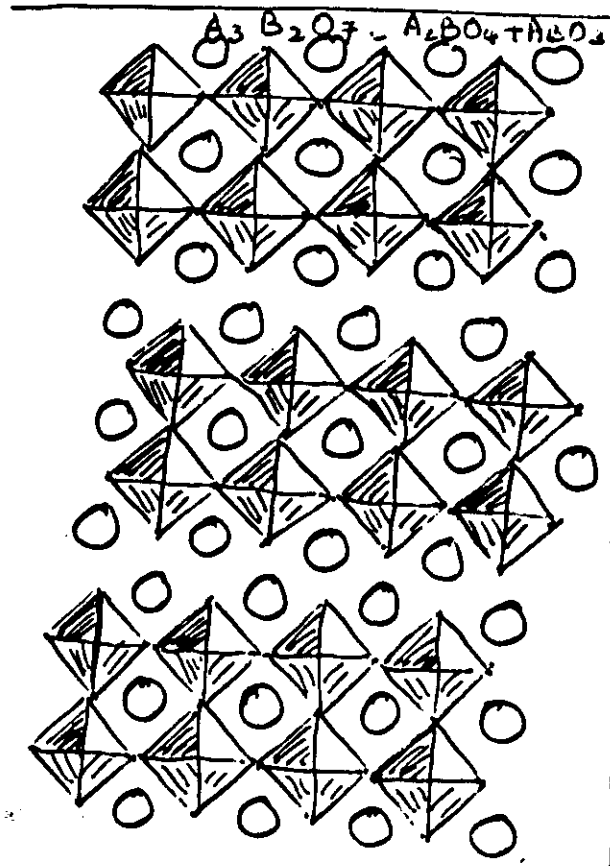

$Ba_3B_2O_7 - A_2BO_4 + ABO_3$

e.g. $La_3Ni_2O_7$, $Sr_3Ti_2O_7$

$La_2SrCu_2O_6$

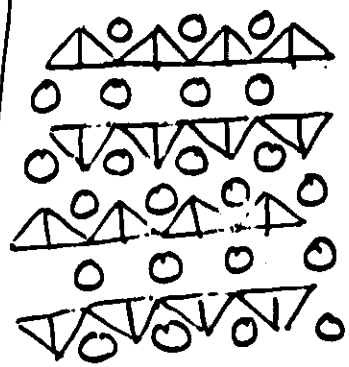

$La_3Cu_2O_{7-\delta}$

$La_4Cu_3O_{10-\delta}$

etc ?

PGI 16

Aurivillius phases

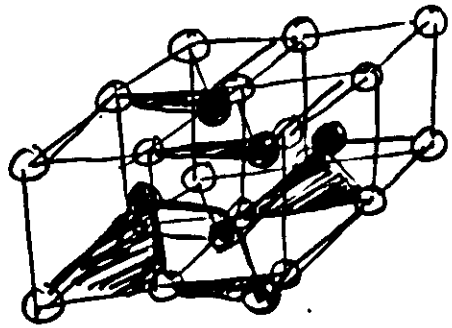

Bi_2WO_6

$Bi_3W_2O_9$

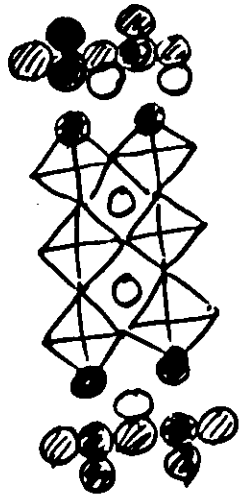

Bi_2O_2

$Bi_2Ti_3O_{10}$

$(Bi_2O_2)(A_nB_{n+1}O_{3n+1})$

$(Bi_2O_2)(A_{n-1}B_nO_{3n+1})$

$Bi_{14}Ti_3O_{12}$

$Bi_9Ti_6CrO_{24}$

$Bi_4Ti_3O_{12}.Bi_5Ti_3CrO_{15}$

ordered intergrowth

$(Bi_4Ti_3O_{12})(BaBi_4Ti_4O_{15})$

see CNR Rao, J. Gopalakrishnan K. Vidyasagar Ind. J. Chem. 23A, 265 (1984) and references therein

PC I 18

Perovskite chains

NO_6 octahedra face-shared

YO_8 Cubes

Y_3MO_7

(tetragonal bronze)

M_5O_{15} units

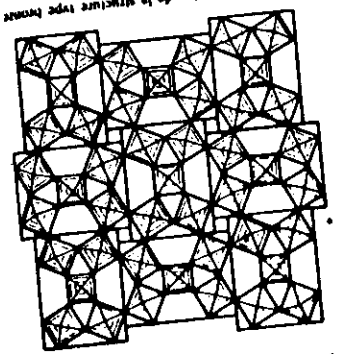

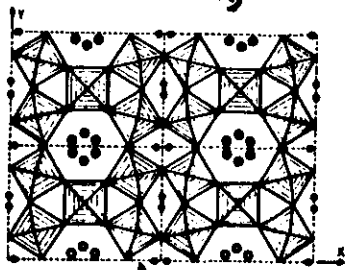

$Ca_2TlTa_5O_{15}$

hexagonal

perovskite layers

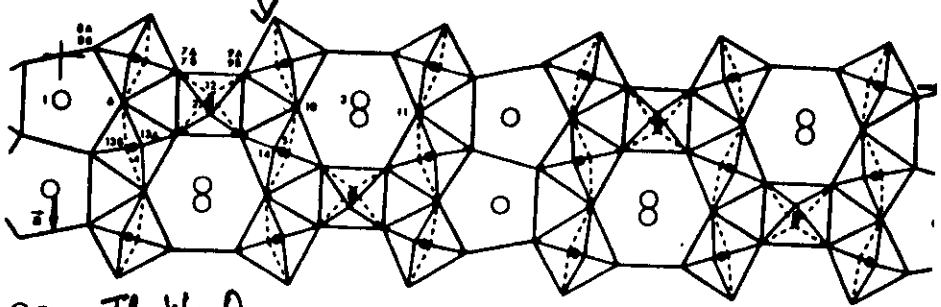

$Tl_2W_4O_{11}$

FIG. 2. $Tl_2W_4O_{11}$. Projection of the structure onto (001). Only one layer of $[WO_6]$ octahedra is drawn.

PC I 17

layering by introduction of PO_4 tetrahedra in WO_3

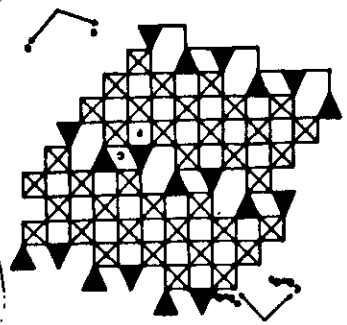

$AP_4W_{12}O_{44}$

HERVIEU AND RAVEAU

which can be considered as replacing two octahedra in the ReO_3-type structure. The c parameter is parallel to the rows of distorted hexagonal tunnels and will only depend on the a_{ReO_3} parameter. Thus the translation between these parameters and those of ReO_3 are given by the following relations:

$$b = a_{ReO_3}, \quad (2)$$

$$c = a_{ReO_3}\sqrt{3}, \quad (3)$$

$$\cos\beta = -1/3, \quad \beta = 116°57'. \quad (4)$$

This framework is favorable for an electron microscopy study since it forms tunnels parallel to b and thus zones of weak electron density which can be distinguished from the zones of high electron density where the files of octahedra and tetrahedra are located. Three sorts of tunnels are located. Motreover, two of them are empty: the perovskite tunnels P located in the ReO_3-type slabs, and the C tunnels formed by two tetrahedra and two octahedra and located at the boundary of the ReO_3-type slabs. The distorted hexagonal

perovskite slab is obtained for strings of m corner-sharing octahedra limited in the same way by one PO_4 tetrahedron at each end. If we choose the "a" parameter of the monoclinic cell of these oxides as a characteristic of width of the ReO_3-type slabs, i.e., parallel to $[001]_{hex}$, its ideal value will be

FIG. 1. Idealized drawing of the monoclinic structure of $AP_4W_{12}O_{44}$ ($m = 6$) projected onto the (010) plane. The black triangles represent PO_4 groups.

Tl_2O_{12} is the only layered bismuth chemical composition of the new compound which consists of these two

Two or Three layered

with F^-

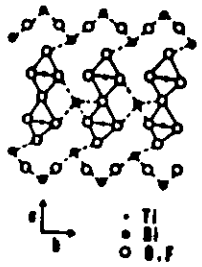

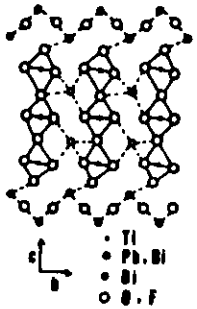

$PbBi_2Ti_2O_8F$ (Aurivillius

FIG. 1a. A section of the proposed structure of $PbBi_2Ti_2O_8F$.

FIG. 1b. A section of the proposed structure of $PbBi_4Ti_4O_{15}F$.

PG I 19

DISORDERED INTERGROWTH IN Sr_2TiO_4

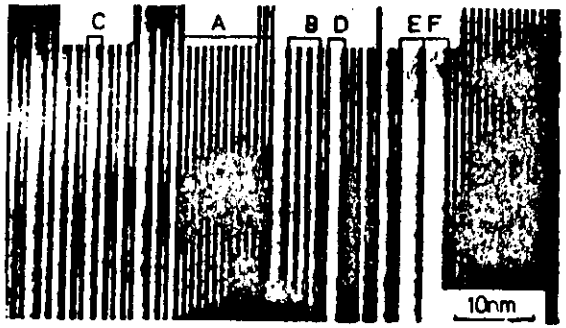

Plate 9—Lattice image of an oxide in the Sr – Ti – O system showing disordered intergrowth among different members of the $Sr_{n-1}Ti_nO_{3n+1}$ family. A, $n=2$; B, $n=3$; C, $n=4$; D, $n=5$; E, $n=7$; and F, $n=8$ (from ref. 89)

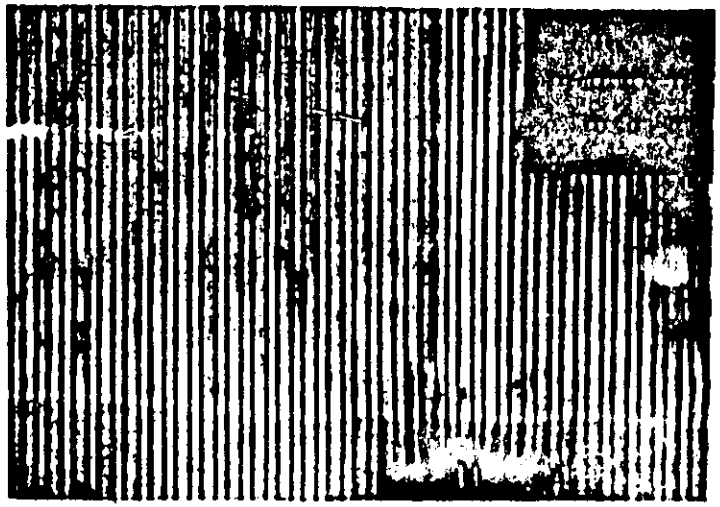

Plate 10—One-dimensional lattice image of $Bi_4Ti_4CrO_{12}$ showing ordered intergrowth between $n=3$ and $n=4$ members of the Aurivillius family.

$Bi_9Ti_6CrO_{27}$

PG I 20

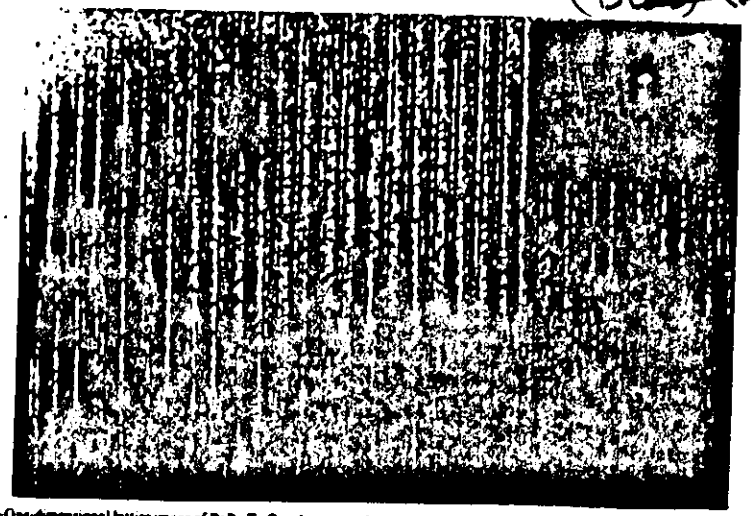

$Ba_4Bi_8Ti_9O$

Plate 11—One-dimensional lattice image of $BaBi_4Ti_4O_{15}$ showing ordered intergrowth of $n=3$ and $n=4$ members of the Aurivillius family.

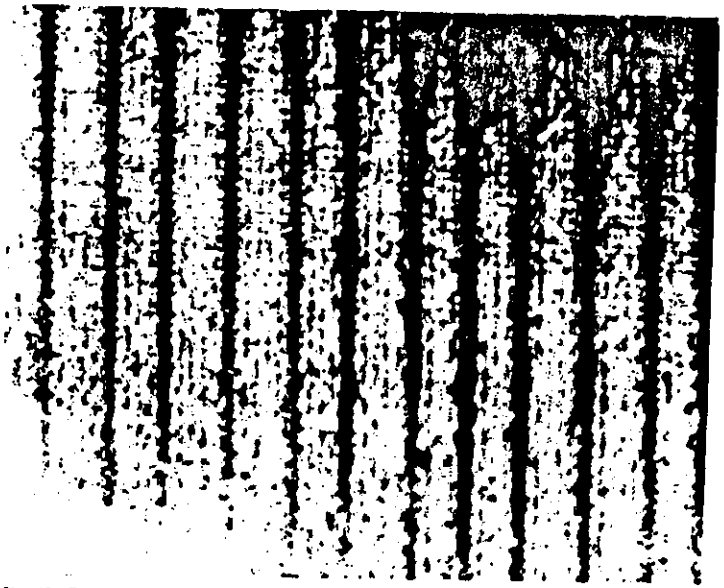

$Bi_9Ti_5Fe_5O_{27}$

Plate 12—Disordered intergrowth of Aurivillius phases as illustrated in the case of $Bi_9Ti_5Fe_5O_{27}$ (from ref. 91).

DISORDERED INTERGROWTH IN LAYERED PEROVSKITES